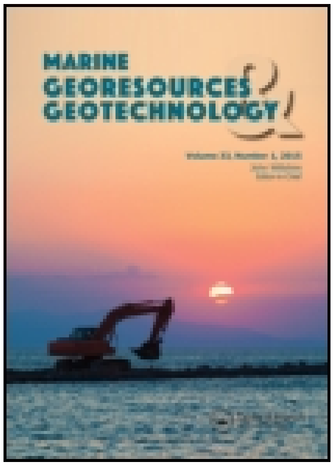

Marine Georesources & Geotechnology
Publication details, including instructions for authors and subscription information:
http://www.tandfonline.com/loi/umgt20

Evaluation of Excess Pore Water Pressure Characteristics in Sand Mat Used for Recycling Dredged Soil

Min-Sun Lee[ab] & Kazuhiro Oda[a]
[a] Department of Civil Engineering, Graduate School of Engineering, Osaka University, Osaka, Japan
[b] Hydro-soft Technology Institute, Japan
Published online: 26 Feb 2015.

To cite this article: Min-Sun Lee & Kazuhiro Oda (2015) Evaluation of Excess Pore Water Pressure Characteristics in Sand Mat Used for Recycling Dredged Soil, Marine Georesources & Geotechnology, 33:5, 367-375, DOI: 10.1080/1064119X.2014.890985

To link to this article: http://dx.doi.org/10.1080/1064119X.2014.890985

Marine Georesources & Geotechnology, 33: 367–375

ISSN: 1064-119X print/1521-0618 online
DOI: 10.1080/1064119X.2014.890985

Evaluation of Excess Pore Water Pressure Characteristics in Sand Mat Used for Recycling Dredged Soil

MIN-SUN LEE[1,2] and KAZUHIRO ODA[1]

[1]*Department of Civil Engineering, Graduate School of Engineering, Osaka University, Osaka, Japan*
[2]*Hydro-soft Technology Institute, Japan*

Received 5 September 2012, Accepted 15 January 2014

The design of sand mats should be reviewed on the basis of excess pore pressure behavior, which can be obtained by combining the characteristics of soft ground with the permeability of the mats. In this study, a banking model test was performed using dredged sand as the mat material to investigate the hydraulic gradient distribution of sand mats. The results were compared with numerical analysis results utilizing Terzaghi's one-dimensional consolidation equation. The results showed that the pore pressure was influenced by an increase in the amount of settlement at the central part of the sand mat as the height of the embankment increased. The measured decrease of the pressure head due to the residing water pressure in the sand mat was delayed compared to the numerical analysis results. Accordingly, sand mats should be laid to reduce the increased hydraulic gradient at the central part of the embankment.

Keywords: dredged soil, excess pore water pressure, hydraulic gradient, model test, sand mat

Introduction

Sand mats are used as a horizontal drainage method for embankments to facilitate the initial consolidation settlement resulting from the weakness of the surface layer at dredged and reclaimed sites. This construction method is applied in areas generally consisting of soft soils.

Reduced fish stocks and other imbalances in coastal ecosystems caused by excessive sand collection in coastal regions have become significant social and environmental issues. In particular, there is an urgent need to procure alternative materials to sand owing to insufficient amounts of sand in reclaimed coastal areas and areas of soft soil ground. This has increased the need for research on using quality dredged soil as a replacement for sand material.

Generally, the construction of a sand mat on soft soil ground serves as an upper drainage layer for consolidation of soft layers and blockage of the ascending groundwater and as a support layer to secure space for construction machinery. Because a sand mat has a significant effect on the consolidation settlement as an upper drainage layer, it is required to have permeability with sufficient drainage capacity. Vertical drains are especially important for facilitating drainage of clay; thus, material particle size criteria are strictly enforced.

Address correspondence to Min-Sun Lee, Department of Civil Engineering, Graduate School of Engineering, Osaka University, 2-1 Yamadaoka, Suita, Osaka, 565-0871, Japan. E-mail: minsoni@civil.eng.osaka-u.ac.jp

Color versions of one or more of the figures in the article can be found online at www.tandfonline.com/umgt.

In order to determine whether dredged soil is a suitable alternative for use as a replacement material for sand mats, a large sample of dredged soil was collected for analyses of physical properties and permeability testing. Representative dredged soil samples (i.e., samples with permeability coefficients that fit the criteria for a sand mat) were selected on the basis of the initial analyses, and a model test was conducted to determine the soil's applicability for use as sand mat material. The excess pore water pressure distribution and sand mat drainage, which are factors necessary to improve the soft soil ground, were quantified. The amount of consolidation settlement according to the embankment load was measured in order to perform a finite element method (FEM) analysis and predict the sand mat's behavior. After consolidation was completed by the final load, a discharge test was performed, and the effects of the permeability were observed. Overall, the aim of this study was to conduct a theoretical review of the design of sand mats and propose a testing technique that can be utilized to improve the adoption of alternative materials and technologies for sand mat construction.

Theoretical Water Pressure Distribution for a Sand Mat

According to Terzaghi's theory of one-dimensional (1D) consolidation (Terzaghi 1943; Terzaghi and Peck 1967), the pore water pressure of a sand mat laid on soft clay ground generally increases in proportion to the amount of settlement in the clay layer. The increased excess pore water pressure is quickly alleviated during draining from the embankment body because of the permeability of the sand

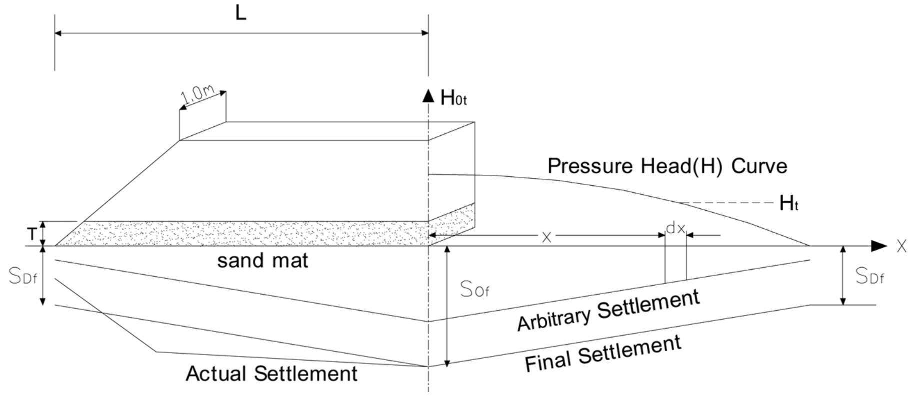

Fig. 1. Distribution of pressure head of sand mat.

mat. However, as shown in Figure 1, if the permeability of the sand mat is low or there is large settlement of the soft clay ground, drainage is delayed in the central part of the embankment and the pressure head is increased.

As shown in Figure 1, the amount of consolidated settlement in the saturated clay layer generated by the embankment load is assumed to undergo a 1D change; the pore water from consolidation is completely drained vertically out of the embankment body in a horizontal direction through the saturated sand mat. Thus, for saturated clay ground, the consolidated settlement of the clay layer can be represented as a function of the average degree of consolidation (U) and time (t) according to Terzaghi's 1D consolidation equation. The pressure head (H) that occurs at a horizontal distance (x) from the sand mat can be calculated with Eq. (1), which is based on Terzaghi's 1D consolidation equation:

$$H = \frac{\gamma_w}{2k \cdot T} \cdot \frac{dU(t)}{dt} \cdot \left(S_{0f} \cdot x - \frac{S_{0f} - S_{Df}}{2L} \cdot x^2 \right) dx \tag{1}$$

where $dU(t)/dt$ is the settlement rate of the clay layer, S_{0f} is the final amount of settlement in the center of the embankment, S_{Df} is the final amount of settlement on the sides of the embankment, T is the thickness of the sand mat, k is the permeability coefficient of the sand mat, $2L$ is the full width of the sand mat, and γ_w is the unit weight of water. Because Eq. (1) assumes a 1D horizontal flow of the pore water from the sand mat, the pressure head is zero ($H = 0$) at the sand mat boundary ($x = L$). Thus, when the maximum pressure head at the center of the embankment is set as H_{0t} and the average pressure head in the transverse distribution is denoted as H_t, the pressure heads can be determined with Eqs. (2) and (3):

$$H_{0t} = \frac{\gamma_w}{2k \cdot H} \left(\frac{S_{0f}}{3} + \frac{S_{Df}}{6} \right) L^2 \cdot \frac{dU(t)}{dt} \tag{2}$$

$$H_t = \frac{\int_0^L h \cdot dx}{L} = \frac{\gamma_w \cdot L^2}{2k \cdot T} \left(\frac{5S_{0f}}{24} + \frac{S_{Df}}{8} \right) \frac{dU(t)}{dt} \tag{3}$$

In Eqs. (2) and (3), the pressure heads of the sand mat vary depending on the settlement rate, the final amount of settlement, the sand mat thickness, the permeability coefficient, and the width of the embankment. Here, the settlement rate can be obtained from the approximation formula of the relationship between the degree of consolidation (U) and time factor (T_v) in Terzaghi's 1D consolidation equation and the measured settlement is given in Eqs. (4) and (5):

$$S_f = \frac{C_c}{1 + e_0} \times H \times \log \frac{P_0 + \Delta p}{P_0} \tag{4}$$

$$U(\%) = \sqrt{\frac{4}{\pi} T_v} = \sqrt{\frac{4}{\pi} \times \frac{C_v \cdot t}{H^2}} = \frac{S_t}{S_f} \times 100 \tag{5}$$

In Eqs. (4) and (5), S_f is the final amount of settlement, S_t is the amount of settlement at an arbitrary time, and the other coefficients are the same as the corresponding symbols in Terzaghi's 1D consolidation equation.

Model Test of the Behavior of Pore Water Pressure in a Sand Mat

Experimental Apparatus and Methods

Figure 2 shows the model test for the hydraulic gradient of the sand mat. For the model test, head devices were designed to be placed on both sides of the soil tank (dimensions: 300 cm × 70 cm × 70 cm) to maintain the groundwater inside the sand mat at a constant level. As shown in Figure 2, four pore water pressure cells, three settlement plates, and two earth pressure cells were installed to measure the amount of settlement of the clay layer and sand mat, and to determine the pore water pressure during embankment loading. The soft clay at the bottom of the sand mat was sufficiently stirred using an electric agitator in a simple soil tank, and the slurry was inserted up to a height of 30 cm while being sealed off from air infiltration. Saturated water was then supplied for approximately 1 week by the head devices until a steady state was reached. Later, a sheet of geo-textile was laid. Dredged soil was spread on this to a height of 20 cm in place of the sand mat. The drainage valves on the left and right sides were closed, and de-aired water was supplied for 1 day. Then, spreading and loading were performed using weathered soil up to the third level. Figure 3 shows the entire view of the model test.

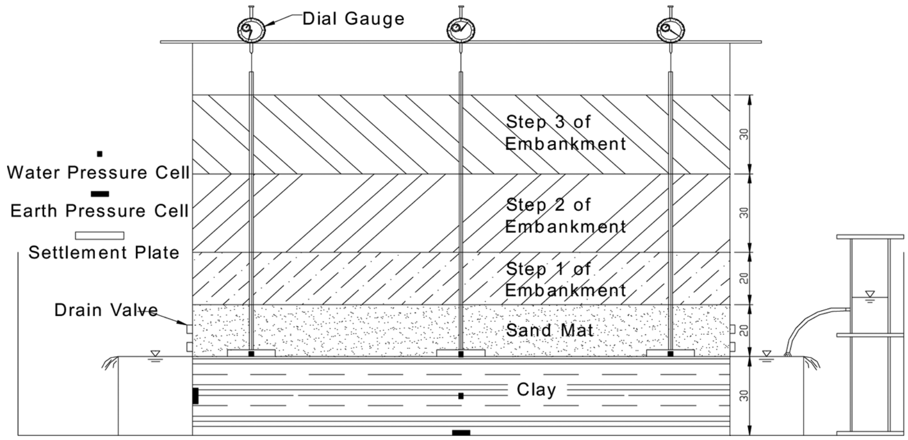

Fig. 2. Model test for hydraulic gradient of sand mat (unit: cm).

Physical and Mechanical Properties of the Sand Mat and Clay

The physical properties and particle distribution of the dredged soil used in this experiment are presented in Table 1 and Figure 4. Figure 4 also contains information on the general particle distribution of sand mats applied in general soft soil ground designs. The dredged soil used in this experiment was slightly poor in terms of sand quality because it was close to the lower limit of the fine materials used for sand mat construction, but it was deemed to be a good alternative to other materials for sand mats in that insufficient aggregate resources by excessive sample collection in coastal regions can be utilized efficiently. In order to examine the consolidation characteristics of the lower clay used in this experiment, a standard consolidation test was performed. The standard consolidation test was run on a specimen of the clay and input characteristics are presented in Table 2.

Table 1. Physical properties of sand mat used in experiment

Water Content (%)	17.6
Plasticity Index (I_p)	NP
Specific Gravity (G_s)	2.60
Passing 75 μm sieve (%)	9.5–13.3
Coefficient of Permeability (cm/sec)	1.34×10^{-3}
USCS	SM

Settlement Characteristics According to Embankment

For the embankment, the degree of consolidation was confirmed to be over 90% using the hyperbolic method (Tan et al. 1991). Loading was performed in three steps up to a height of 100 cm over the course of 11 days. The degree of consolidation according to the settlement of the clay ground was assessed using the ratio of the amount of settlement actually measured with the model test to the final amount of settlement calculated with the specifications of the consolidation test. The final amount of settlement was calculated on the basis of the initial void ratio according to the input moisture content and the ground stress (Δp) that were measured using the earth pressure cell at the bottom of the clay layer. The measured values (Δp) of the earth pressure cell at the center and amounts of settlement (S_{0f} and S_{Df}) measured using the dial gauge at the center and the left

Fig. 3. Whole view of model test.

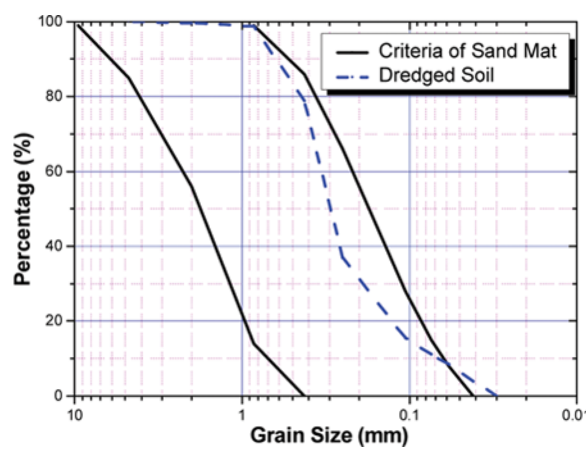

Fig. 4. Pressure head distribution of a sand mat.

Table 2. Physical and mechanical properties of remolded clay

Water Content (w_n, %)		54.5
Unit Weight (γ_t, kN/m^3)		16.6
Specific Gravity (G_s)		2.60
Consolidation	e_0	1.26
	C_c	0.380
	C_s	0.159
	C_v (cm^2/s)	1.56×10^{-4}
	P_c (kPa)	10
USCS		CL

Table 3. Amount of settlement and ground stress measured during embankment

		S_{Df} (cm)	S_{0f} (cm)	Δp (kPa)
Sand Mat		0.89	1.33	3.4
Embankment	Step 1	1.35	1.87	3.6
	Step 2	1.76	2.32	5.1
	Step 3	2.04	2.62	5.1

and right fore-ends in the model test device (Figure 2) during the embankment are presented in Table 3.

Numerical Analysis of Pore Water Pressure of the Sand Mat

Pore Water Pressure According to the Permeability Coefficient and Thickness of the Sand Mat

The settlement rate ($dU(t)/dt$) for the initial degree of consolidation (U) of 3%, obtained with a clay layer thickness of 30 cm and the consolidation coefficient from Table 2, were substituted into Eq. (5); the amounts of settlement at the center of the embankment (S_{0f}) and in the outer part of the embankment (S_{Df}) measured in step 3 of the embankment and a sand mat thickness (T) of 20 cm were substituted into Eq. (2). When the permeability (k) changed by up to 10^{-4}–10^{-2} cm/s, the pressure head H_t was calculated according to the horizontal distance of the sand mat. The results are shown in Figure 5. As shown in the figure, a lower permeability coefficient of the sand mat produced a higher hydraulic gradient at the center of the embankment, which in turn increased the pressure head. In particular, there was a significant increase in the pressure head when the permeability coefficient of the sand mat was below 10^{-4} (cm/s) because this caused a delay in the draining of pore water. In addition, the settlement rate calculated when the degree of consolidation was 3% using Eq. (2), the amount of settlement at the center of the embankment (S_{0f}), and the amount of settlement in the outer part of the embankment (S_{Df}) measured in step 3, are presented in Table 3, where the parameters were substituted into the equation using a permeability coefficient (k) that was maintained at a constant value of 10^{-3} cm/s. Then, the thickness of the sand mat (T) was varied in the range of 5–30 cm to analyze the resulting value of the pressure head. The results from these analyses are shown in Figure 6.

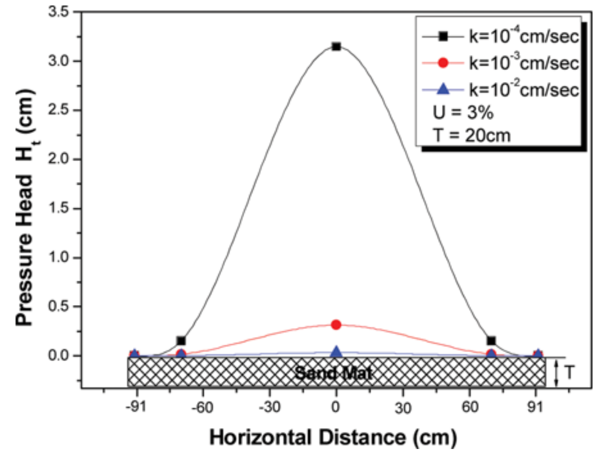

Fig. 5. Pressure head according to changes in permeability coefficient.

Figure 6 shows that an increase in the thickness of the sand mat caused a gradual decrease in the pressure head; the change in the pressure head was small in the outer part of the embankment because it was less affected by the hydraulic gradient. Thus, if the spread thickness of the sand mat is increased while the permeability coefficient is maintained at the same level, the hydraulic gradient decreases and causes a reduction in the pressure head.

Pore Water Pressure of the Sand Mat Based on the Coefficient of Consolidation in the Clay Layer

In order to analyze the pressure head of the sand mat according to the settlement rate of clay at the bottom, the coefficient of consolidation (C_v) was selected as a factor that affects the settlement rate in the clay layer. When the consolidation coefficient (C_v) of the clay layer was changed to be in the range of 10^{-5}–10^{-3} cm^2/s with an initial degree of consolidation (U) of 3%, the consolidation time (t) for the arbitrary consolidation coefficient can be calculated using Eq. (5). Thus, the settlement rate ($dU(t)/dt$) with

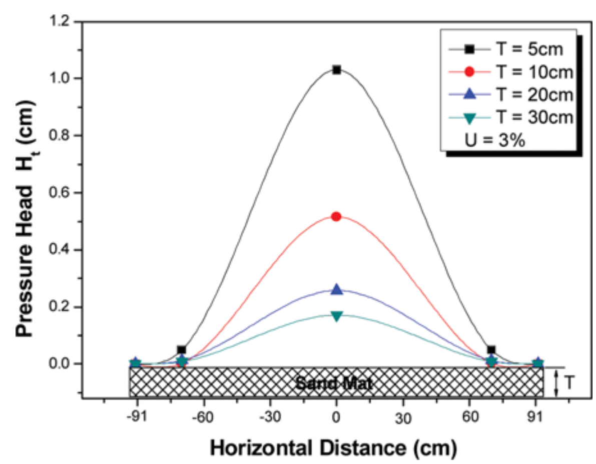

Fig. 6. Pressure head according to changes in thickness of sand mat.

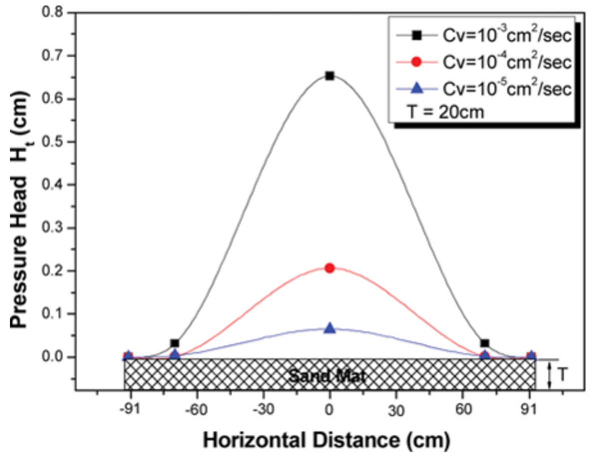

Fig. 7. Pressure head according to changes in consolidation coefficient.

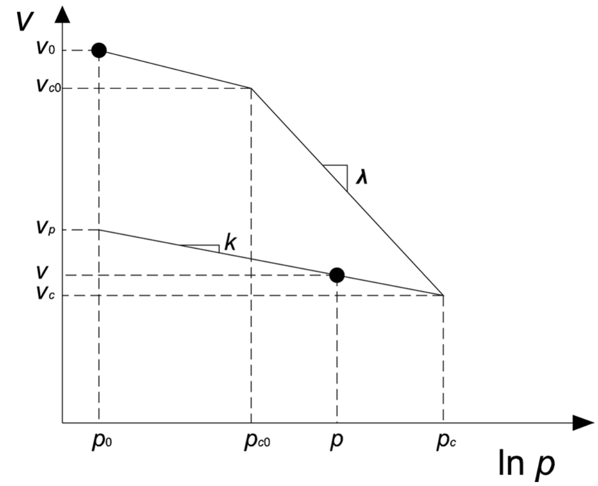

Fig. 8. Logarithmic relations between pressure (p) and specific volume (v).

respect to the degree of consolidation can be obtained. The amounts of settlement at the center of the embankment (S_{0f}) and in the outer part of the embankment (S_{Df}) measured in step 3, as presented in Table 3, and the permeability coefficient (k), which was constant at 10^{-3} cm/s, were substituted into Eq. (2) to obtain the pore water pressure in the sand mat. The results are shown in Figure 7; there was a positive correlation between the consolidation coefficient of the clay layer and the pressure head at the center of the embankment. This was due to the increase in the amount of consolidation drainage resulting from the increased settlement rate of the clay layer, which was caused by increased stress at the center of the embankment.

Analysis and Discussion of Results

Finite Element Method (FEM) Analysis Using the Modified Cam-Clay Model

The FEM analysis was performed in order to predict the consolidation settlement according to the embankment load and the sand mat behavior of the pore water pressure (Snadhu and Wilson 1969). The FEM analysis was conducted using the Modified Cam-Clay model (Mayne 1980; Gens and Potts 1988; Callari et al. 1998). The Modified Cam-Clay model describes the isotropic compression response through linear relations between the specific volume (v) and the logarithm of the pressure (p). These relations can be expressed as follows in Eqs. (6) and (7) (see also Figure 8):

$$v = v_p - \ln\left(\frac{p}{p_0}\right) \quad \text{in the elastic range} \tag{6}$$

$$v_c = v_{c0} - \lambda \ln\left(\frac{p_c}{p_{c0}}\right) \quad \text{in the elasto} - \text{plastic rage} \tag{7}$$

where v_p is the specific volume obtained by unloading the current configuration (p, v) to the initial pressure p_0, and λ is the slopes in the v-ln p plane of the overconsolidation lines and of the normal consolidation line, respectively. The sets (p_{c0}, v_{c0}) and (p_c, v_c) are the pressure and the specific volume pertaining to the initial and the current yielding state, respectively. Some of the consequences relative to the adoption of v-ln p relations were then investigated. Using Figure 8, it is easy to verify the following relation:

$$v_c - v_{c0} = v_p - v_0 - k \ln\left(\frac{p_c}{p_{c0}}\right) \tag{8}$$

where v_0 is the initial specific volume. k is the slopes in the v-ln p plane of the over-consolidation lines and of the normal-consolidation line. Substitution of this relation into the normal consolidation line in Eq. (7) leads to Eq. (9):

$$v_p - v_0 - k \ln\left(\frac{p_c}{p_{c0}}\right) = -\lambda \ln\left(\frac{p_c}{p_{c0}}\right) \tag{9}$$

Excess Pore Water Pressure of the Sand Mat According to the Height of Embankment

The top of Figure 9 shows the results of FEM analysis conducted using the Modified Cam-Clay model of the settlement, as measured using the settlement gauges installed at the central part and on the left and right sides of the sand mat layer, as a function of the time. The bottom of the figure shows the measurements of the pore water pressure cells installed inside the sand mat layer and at the center of the clay layer. As the height of the embankment increased, the increased amount of settlement at the central part of the clay layer was greater than the left and right sides. Because of the soft surface and low shear strength, there was immediate settlement during the laying of the sand mat and primary embankment, and the actual amount of measured settlement was higher than that calculated by FEM analysis.

Afterward, the settlements from the lab measurements and FEM analysis tended to be similar, but the actual settlement amount was slightly smaller owing to the residual pore water pressure caused by inhibited drainage through the influence of differential settlement during the experiment. A comparison of the pore water pressures in the clay and sand mat layers during embankment showed a significant

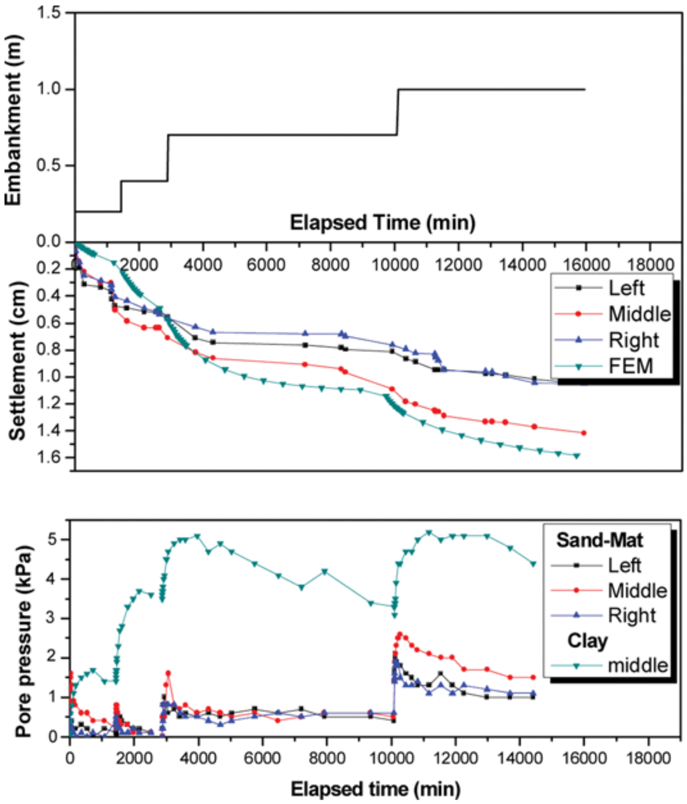

Fig. 9. Pore water pressure of sand mat and settlement and pore water pressure of clay ground.

increase in pore water pressure in the former, whereas such an increase was prominent at the center and small on the left and right sides of the latter. This was due to the increased hydraulic gradient that was caused by an increase in the residual pore water pressure resulting from the concentrated stress in the central part of the clay layer. The excess pore water pressure increased rapidly after loading because of the small permeability coefficient in the clay layer, but it declined over time owing to the permeability of the sand mat. Figures 10–13 show the pore water pressures that were measured with the pore water pressure cells installed in the

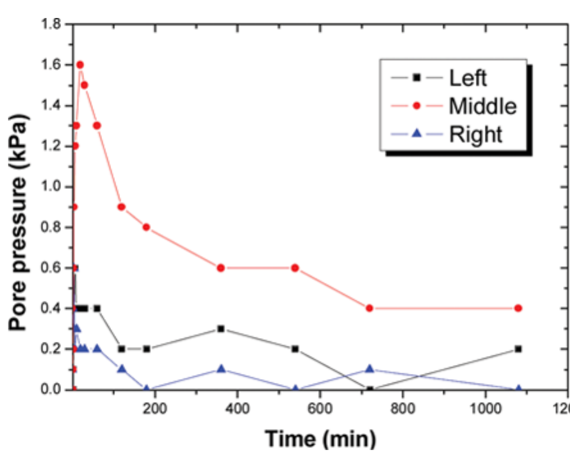

Fig. 10. Changes in pore water pressure during laying of sand mat.

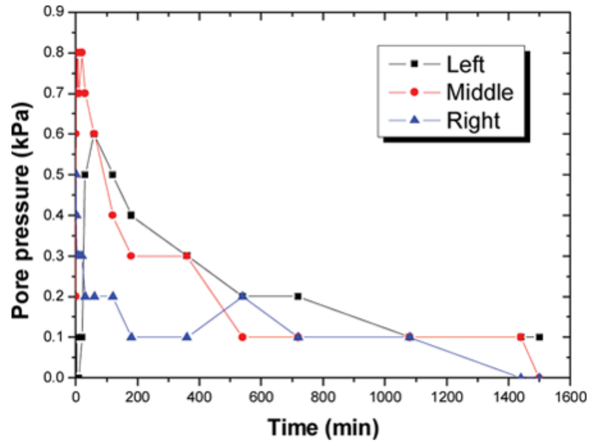

Fig. 11. Changes in pore water pressure during step 1 of embankment.

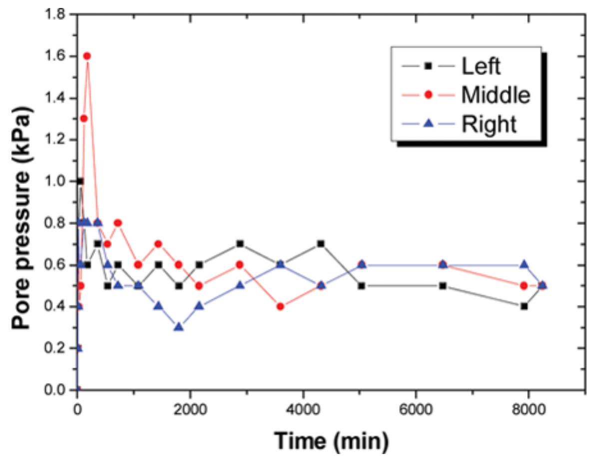

Fig. 12. Changes in pore water pressure during step 2 of embankment.

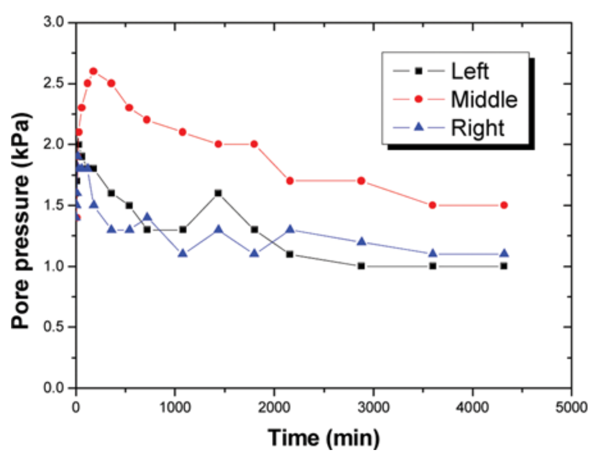

Fig. 13. Changes in pore water pressure during step 3 of embankment.

sand mat and clay layer according to embankment during the model test. Figure 10 shows a rapid increase in pore water pressure caused by soil disturbance; the groundwater level remained above the saturated soft clay layer. The excess pore water pressure increased up to 1.6 kPa at the center of the sand mat and gradually decreased over time until it reached 0.6–0.4 kPa after 400 min. Moreover, the excess pore water pressure in both drainage areas increased slightly before rapidly declining. Figure 11 shows the measured pore water pressure during the primary embankment; it increased slightly at the center to a maximum of 0.8 kPa and increased greatly on the left and right sides to a maximum of 0.6 kPa. When the sand mat was laid, the clay layer underwent a gradual transition from an unstable state to a stable state and normal consolidated settlement occurred. Figure 12 shows the pore water pressure measured during step 2 of embankment. The excess pore water pressure at the center increased up to 1.6 kPa during the initial laying before decreasing to approximately 0.5 kPa over time. The bottom clay foundation subsided uniformly until step 2 of embankment, which showed that the sand mat maintained its horizontal function.

The changes in the pore water pressure of the sand mat at the time of final embankment revealed a significant increase in excess pore water pressure at the central part of up to 2.6 kPa and for the left and right sides of up to 2 kPa during initial laying from those in step 2 (Figure 13). Over time, the pore water pressure at the central part of the sand mat was observed to be higher than that for the left and right sides with a constant slope. The settlement amount increased at the center of the embankment and the sand mat formed a concave shape, which caused the pore water to form a pool because it could not be drained out.

Pressure Head of the Sand Mat According to the Degree of Consolidation in the Clay Layer

Figures 14 and 15 show a comparison of the measured results and the numerical analysis results of the pore water pressures according to degree of consolidation during steps 2 and 3 of embankment.

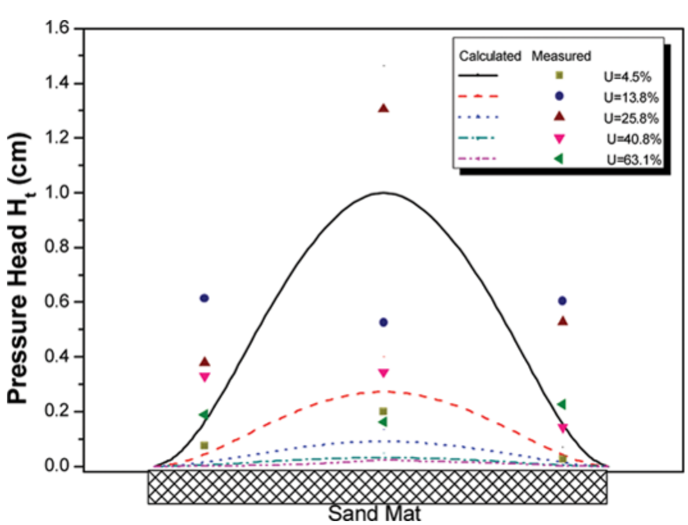

Fig. 14. Comparison of measured results and numerical analysis results of pore water pressure according to degree of consolidation during step 2 of embankment.

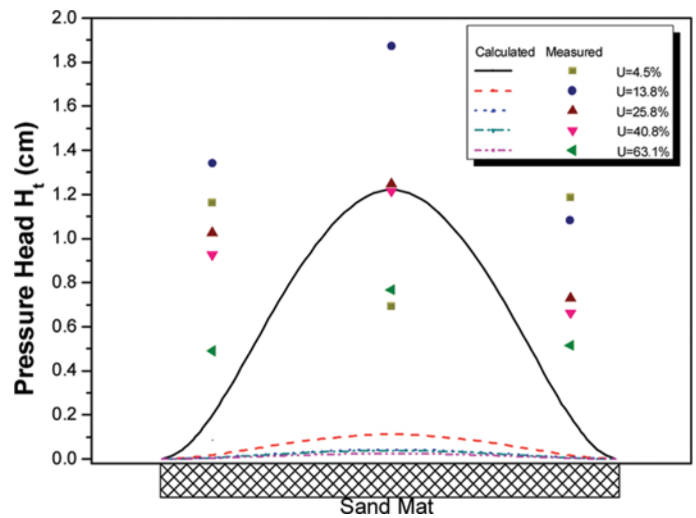

Fig. 15. Comparison of measured results and numerical analysis of pore water pressure according to degree of consolidation during step 3 of embankment.

The thickness and consolidation coefficient of the clay layer in the experiment were substituted into Eq. (5) to obtain the settlement rate ($dU(t)/dt$) with respect to the predetermined degree of consolidation; this was then substituted into Eq. (2) to calculate the pressure head. The amount of settlement according to the embankment was obtained from Table 3. The degree of consolidation of the clay ground was obtained using the ratio of the amount of settlement (S_t) measured through the model test to the final amount of settlement (S_f) calculated using Eq. (4). The pore water pressures of the laboratory clay ground corresponding to the predetermined degree of consolidation are shown in Figures 14 and 15. An analysis of steps 2 and 3 of embankment, which caused a significant increase in the excess pore water pressure, showed that the excess pore water pressure of the sand mat measured during step 2 of embankment in the model test was generally higher than the corresponding numerical analysis results owing to the increase in the degree of consolidation.

The measured excess pore water pressure was at its maximum at the center of the mat when the degree of consolidation was 26% and on the left and right sides when the degree of consolidation was 14%. On the other hand, the numerical analysis results revealed that the maximum excess pore water pressure was reached when the degree of consolidation was 5%. Figure 15 shows that the pore water pressure was measured at its maximum at the center during step 3 of embankment when the degree of consolidation was 14% and on the left and right sides when the degree of consolidation was 5% and 14%. On the other hand, the numerical analysis results revealed that the maximum excess pore water pressure was reached when the degree of consolidation was 5%, just as with step 2 of embankment. For step 3 of embankment, where the height of the embankment was greater, the excess pore water pressures measured for the left

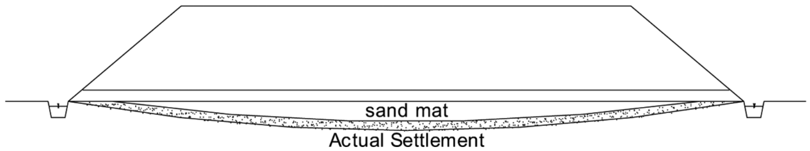

Fig. 16. Section of embankment during final settlement.

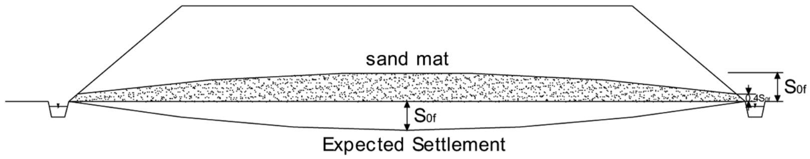

Fig. 17. New sand mat construction method.

and right sides were higher than those measured during step 2 of embankment. With an increase in the degree of consolidation, the measured values for the left and right sides of the sand mat were greater than the numerical analysis results. As the embankment grew taller, the settlement amount increased in the central part of the sand mat; this caused deformation, which inhibited drainage. Thus, the amount of settlement on the central, left, and right sides should be predicted prior to the laying of the sand mat in order to reduce the hydraulic gradient and horizontal water head resistance in the sand mat.

Proposed Sand Mat Construction Method

Generally, the thickness of the sand mat laid on a clay ground differs depending on the calculation performed to ensure space for construction equipment and settlement of the soft soil ground. However, the general thickness was approximately 50 cm regardless of the lateral ditch or central part. However, when embankment was performed after the laying of the sand mat, the central part showed a great deal of settlement, as shown in Figure 16; this impeded drainage and caused interstitial water to remain. Thus, a construction method for sand mats is proposed here based on the findings of this study (Figure 17). Figure 17 shows that the conventional method for laying the sand mat results in a large increase in settlement because of the stress concentrated in the central part of the embankment, and a concave shape is formed as the sand mat subsides below the surface with the same amount of settlement. Thus, laying the sand mat to be equal to the amount of settlement that is predicted to occur during embankment can ensure that the horizontal gradient of the interstitial water from consolidated sediments will be maintained during maximum settlement and will enable drainage in the lateral ditch.

Furthermore, as shown in Figure 14, when the pressure head is at its maximum at the center, the pressure head at the lateral ditch is about 38% that of the center. Because the pressure head and sand mat thickness are proportional, as shown in Eq. (3), horizontal drainage can be maintained when the sand mat has a thickness of 40% that of the center.

Conclusions

In this study, the pressure head distribution of a sand mat laid on a clay layer was analyzed based on Terzaghi's theory of 1D consolidation, which takes into consideration the settlement characteristics of the bottom clay layer. In addition, the effect of the settlement characteristics of the soft clay layer on the excess pore water pressure distribution of the upper sand mat layer was reviewed via a model loading test. On the basis of the results, a new sand mat construction method was proposed. The findings of this study can be summarized as follows:

1. The pressure head equation, which considers the settlement rate in the clay layer to the settlement amount using Terzaghi's 1D consolidation equation, was highly influenced by the permeability coefficient and thickness of the sand mat, and the consolidation coefficient of the clay layer.
2. Because the settlement level of the embankment center increased the pressure head, it reduced the horizontal drainage of the sand mat.
3. The excess pore water pressure of the sand mat measured during steps 2 and 3 of embankment in the model test was at its maximum at the center when the degree of consolidation in the clay layer was 26% or 14% and on the left and right sides of the sand mat when the degree of consolidation was 14%. In the numerical analysis, the maximum excess pore water pressure was attained when the degree of consolidation was 5%.
4. The reason for the delay in the decrease of the pressure head measured during the test relative to the numerical analysis results was the increased hydraulic gradient that occurred because the increased settlement amount at the central part was transferred to the left and right sides of the mat.
5. In order to reduce the horizontal hydraulic gradient that occurs due to the increased settlement at the center of the embankment and maintain horizontal drainage, the sand mat should be laid in an amount equal to the amount of settlement predicted to occur, with the sand mat in the lateral ditch having a thickness of 40% that of the center, as shown in Figure 17.

References

Callari, C., F. Auricchio, and E. Sacco. 1998. A finite-strain cam-clay model in the framework of multiplicative elasto-plasticity. *International Journal of Plasticity* 14(12): 1155–1187.

Gens, A. and D. M. Potts. 1988. Critical state models in computational geomechanics. *Engineering Computations* 5(3): 178–197.

Mayne, P. W. 1980. Cam-clay predictions of undrained strength. *Journal of Geotechnical and Geoenvironmental Engineering ASCE* 106(GT11): 1219–1242.

Snadhu, R. S. and E. L. Wilson. 1969. Finite element analysis of seepage in elastic media. *Journal of the Engineering Mechanics Division ASCE* 95(EM3): 641–651.

Tan, T. S., T. Inoue, and S. L. Lee. 1991. Hyperbolic method for consolidation analysis. *Journal of Geotechnical Engineering* 117(11): 1723–1737.

Terzaghi, K. 1943. *Theoretical Soil Mechanics*. New York: John Wiley and Sons.

Terzaghi, K. and R. B. Peck. 1967. *Soil Mechanics in Engineering Practice.* 2nd ed. New York: John Wiley and Sons.